Multiple relaxation time lattice Boltzmann schemes for advection-diffusion equations with application to radar image processing

Jordan Michelet [a,b,*], Mohamed Mahdi Tekitek [b], Michel Berthier [b]

[a] *Bowen Company, Av. du Canada, 91 940 Les Ulis, France*
[b] *MIA Laboratory, La Rochelle Université, Av. Albert Einstein, BP 33 060, 17 031 La Rochelle, France*

ARTICLE INFO

ABSTRACT

Motivated by marine radar image processing, we investigate the accuracy of multiple relaxation time lattice Boltzmann schemes designed to simulate two-dimensional convection-diffusion equations. The context of application requires to deal with non-constant advection velocity. Using Taylor expansions, instead of the widely used Chapman-Enskog expansions, we show how to control the accuracy of these schemes when deriving equivalent partial differential equations. On the one hand, a third order analysis is conducted on a scheme involving a constant advection velocity and no source term. First, this analysis derives the stability region through the von Neumann analysis. Second, a numerical convergence rate of three is obtained thanks to an appropriate choice of parameters. On the other hand, non-constant advection velocity together with non-zero source term, introduce additional terms at the second order. Regarding the targeted application, these extra terms are shown to be negligible and experiments on real data show that such multiple relaxation time lattice Boltzmann schemes are relevant for marine radar denoising and enhancement.

© 2022 Elsevier Inc. All rights reserved.

1. Introduction

Lattice Boltzmann (LB) schemes are obtained by considering Boltzmann's equation with a discretized phase space. There are essentially two ways to handle Boltzmann's collision operator when designing such schemes. The first one makes use of the Bhatnagar-Gross-Krook (BGK) collision operator defined from an equilibrium distribution [2]. Alternatively, the collision can be performed in a moment space by introducing several relaxation times. This second way leads to Multiple Relaxation Time (MRT) schemes [8]. BGK schemes can be considered as a particular case of MRT LB schemes with a Single Relaxation Time (SRT).

The LB methods are widely used for simulations, for instance in computational fluid dynamics, acoustics, thermals or magnetohydrodynamics. In what follows, the focus is on the more specific and less frequently addressed problem of simulating Convection-Diffusion equation (CDE) possibly with non-constant advection velocity and non-linear reaction term [21,4,7,10,16,17,22,25]. In order to study the consistency of the corresponding LB schemes, one has to compute expansions from the discretized Boltzmann equation to obtain the so-called equivalent Partial Differential Equation (PDE) that approximates the initial governing PDE up to a given order. The most used expansions are the Chapman-Enskog ex-

---

pansions [5] that require to introduce various time/space scales. To skip handling these latter, one can use usual Taylor expansions at the acoustic scale in the moment space [9]. In the following, this second strategy is adopted.

Although they appear more complex, MRT LB schemes have significant advantages over simple SRT LB schemes, which explain their growing popularity. They include for instance cumulant [11] and entropic [14] LB schemes. They also allow for better handling of boundary conditions [15] and physical quantities [8]. Their key feature used in this work is that they are much more stable than SRT LB schemes, as illustrated in our specific application to marine radar image processing, see also [20].

Actually, the design of LB schemes for image processing is still a widely open challenge. It is clear that their easy parallel implementation for real time processing could improve many of PDE-based existing algorithms. We refer to [6,12,23,24,26] for contributions using SRT LB schemes, and to [20] for the sole, up to our knowledge, contribution using a MRT LB scheme in this context.

Let us explain briefly the way CDE are involved in marine radar image processing. The images to be processed are Range-Doppler Map (RDM) which allow visualizing radar signals in the frequency domain. They are highly corrupted by an interference noise, have low contrast, and the objects to be detected have no apparent contours. A first process is applied by means of a Chan-Vese k-phase diffuses interface motion model to reduce the noise induced by the sea clutter, see [18] for details. The advection velocity is then chosen to be the gradient of the resulting image, whereas the diffusion and reaction are given by the Allen-Cahn equation [1]. The so-obtained PDE is used to improve the denoising with the diffusion, and to enhance the signal of interest with the advection.

Let summarize the main contributions of this work as follows. We give an explicit derivation up to the second order of the equivalent PDE of a governing CDE with non-constant advection velocity and non-zero source term. This derivation is performed using Taylor expansions in the moment space of a MRT D2Q9 LB scheme. We give an explicit derivation of the equivalent PDE up to the third order when the advection velocity is constant and there is no source term. From a theoretical point of view, a suitable choice of relaxation times increases the scheme accuracy to order three. Using this choice of relaxation times, we performed a von Neumann analysis to derive the stability region depending on the Péclet number Pe, the Courant number Cr, and the time step Δt. Within the stability region, a numerical convergence rate of three is obtained and validated thanks to an appropriate choice of LB parameters from a test case for which the analytical solution is known. We propose a marine radar image processing algorithm implemented by means of a MRT D2Q9 LB scheme that simulates a CDE to denoise RDM and to enhance the signal of interest. Experiment results on real data are presented and validate the relevance of the algorithm. We also show that this kind of image processing requires the use of MRT instead of SRT D2Q9 LB schemes, since the latter lack of stability.

This paper is organized as follows. Section 2 is devoted to recalls about MRT D2Q9 LB schemes. Section 3 contains the derivation of the equivalent PDE up to the second order of a governing CDE with non-constant advection velocity and non-zero source term. The particular case of constant advection velocity and null source term is detailed in Section 4 up to the third order. Applications to marine radar image processing are presented in Section 5.

2. MRT D2Q9 LB schemes

The application to marine radar image processing presented later requires to simulate a two-dimensional CDE of the form

$$\frac{\partial}{\partial t} U\left(\vec{x}, t\right) + \vec{\nabla} \cdot \left(\vec{w}\left(\vec{x}\right) U\left(\vec{x}, t\right)\right) - D \Delta U\left(\vec{x}, t\right) = S\left(\vec{x}, t\right), \tag{1}$$

with a constant diffusion coefficient D, possibly a non-constant advection velocity $\vec{w}\left(\vec{x}\right)$ and a non-linear source term $S\left(\vec{x}, t\right)$. The proposed LB scheme makes use of the D2Q9 lattice $\mathcal{L}$ (see Fig. 1) defined by

$$\vec{v}_i = \lambda \vec{e}_i = \lambda \begin{cases} (0,0) & i = 0 \\ (\pm 1, 0), \ (0, \pm 1) & i = 1, 2, 3, 4 \\ (\pm 1, \pm 1) & i = 5, 6, 7, 8 \end{cases}, \tag{2}$$

where $\lambda = \Delta x / \Delta t$ is the numerical lattice velocity, and Δx and Δt are the space step of the lattice and the time step, respectively. The discretized Boltzmann's equation with a forcing term writes [15]

$$f(\vec{x} + \vec{v}_i \Delta t, \vec{v}_i, t + \Delta t) = f^*(\vec{x}, \vec{v}_i, t) + \Delta t F(\vec{x}, \vec{v}_i, t), \tag{3}$$

or equivalently [9]

$$f(\vec{x}, \vec{v}_i, t + \Delta t) = f^*(\vec{x} - \vec{v}_i \Delta t, \vec{v}_i, t) + \Delta t F(\vec{x} - \vec{v}_i \Delta t, \vec{v}_i, t), \tag{4}$$

where f^* is the distribution after collision. Let us denote $f_i\left(\vec{x}, t\right) := f(\vec{x}, \vec{v}_i, t)$, $F_i\left(\vec{x}, t\right) := F(\vec{x}, \vec{v}_i, t)$, $\vec{f} := (f_0, f_1, \ldots, f_8)$, and $\vec{F} := (F_0, F_1, \ldots, F_8)$. The solution $U\left(\vec{x}, t\right)$ of (1) and the distributions $f_i\left(\vec{x}, t\right)$ are related by
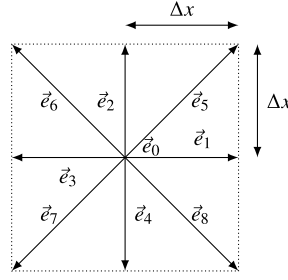
Fig. 1. The D2Q9 lattice.

Table 1
D2Q9 equilibrium of non-conserved physical moments as function of the single conserved moment U.

Physical moment	j_x	j_y	E	p_{xx}	p_{xy}	q_x	q_y	χ
Equilibrium	$\lambda \alpha_{j_x}$	$\lambda \alpha_{j_y}$	$\lambda^2 \alpha_\text{E}$	$\lambda^2 \alpha_{\text{p}_{xx}}$	$\lambda^2 \alpha_{\text{p}_{xy}}$	$\lambda^3 \alpha_{j_x} \alpha_{q_x}$	$\lambda^3 \alpha_{j_y} \alpha_{q_y}$	$\lambda^4 \alpha_\chi$

$$U\left(\vec{x}, t\right) = \sum_{i=0}^{8} f_i\left(\vec{x}, t\right). \tag{5}$$

As mentioned earlier, MRT LB schemes deal with collision in a moment space [8]. Let us recall briefly how to define the linear transform

$$\vec{m}\left(\vec{x}, t\right) = \boldsymbol{M} \vec{f}\left(\vec{x}, t\right) \quad \Longleftrightarrow \quad \vec{f}\left(\vec{x}, t\right) = \boldsymbol{M}^{-1} \vec{m}\left(\vec{x}, t\right) \tag{6}$$

between moment vector $\vec{m}\left(\vec{x}, t\right)$ and distribution vector $\vec{f}\left(\vec{x}, t\right)$. Regarding our specific application, the nine physically relevant moments are the only one conserved moment $U\left(\vec{x}, t\right)$ together with the eight moments defined by

$$j_x\left(\vec{x}, t\right) \text{ and } j_y\left(\vec{x}, t\right) \text{ with } \vec{j}\left(\vec{x}, t\right) = \sum_{i=0}^{8} \vec{v}_i f_i\left(\vec{x}, t\right),$$

$$\text{E}\left(\vec{x}, t\right) = \sum_{i=0}^{8} \frac{\left\|\vec{v}_i\right\|^2}{2} f_i\left(\vec{x}, t\right), \quad \text{p}_{xx}\left(\vec{x}, t\right) = \sum_{i=0}^{8} \left(v_{i,x}^2 - v_{i,y}^2\right) f_i\left(\vec{x}, t\right), \quad \text{p}_{xy}\left(\vec{x}, t\right) = \sum_{i=0}^{8} v_{i,x} v_{i,y} f_i\left(\vec{x}, t\right),$$

$$q_x\left(\vec{x}, t\right) \text{ and } q_y\left(\vec{x}, t\right) \text{ with } \vec{q}\left(\vec{x}, t\right) = \sum_{i=0}^{8} \vec{v}_i \frac{\left\|\vec{v}_i\right\|^2}{2} f_i\left(\vec{x}, t\right), \quad \chi\left(\vec{x}, t\right) = \sum_{i=0}^{8} \frac{\left\|\vec{v}_i\right\|^4}{4} f_i\left(\vec{x}, t\right). \tag{7}$$

The matrix $\boldsymbol{M}$ of the linear transformation is determined by requiring that these moments can be written as linear combinations $\sum_{i=0}^{8} p_k\left(\vec{v}_i\right) f_i\left(\vec{x}, t\right)$ with p_k in $\mathbb{R}[X, Y]$. Applying Gram-Schmidt orthogonalization, one obtains the set of polynomials $(p_0, p_1, \ldots, p_8)$ defined by $\left(1, \ X, \ Y, \ 3\left(X^2 + Y^2\right) - 4\lambda^2, \ X^2 - Y^2, \ XY, \ X\left(3\left(X^2 + Y^2\right) - 5\lambda^2\right),\right.$ $Y\left(3\left(X^2 + Y^2\right) - 5\lambda^2\right), \ 9\left(X^2 + Y^2\right)^2 /2 - 21\lambda^2 \left(X^2 + Y^2\right)/2 + 4\lambda^4\right)$, and the matrix $\boldsymbol{M}$ defined by $M_{k,i} = p_k(\vec{v}_i)$. The vector $\vec{\mathbb{F}}\left(\vec{x}, t\right) = \boldsymbol{M} \vec{F}\left(\vec{x}, t\right)$ is a forcing vector expressed in the moment space. Therefore, $\mathbb{F}_k$, the kth component of $\vec{\mathbb{F}}$, is the force applied to the moment m_k and $\mathbb{F}_0$ is the contribution of the source term $S\left(\vec{x}, t\right)$. The collision in the moment space involves different relaxation times s_k and equilibrium moments m_k^{eq} and is described by the equation

$$m_k^* = (1 - s_k) m_k + s_k m_k^{eq}, \tag{8}$$

for $k = 1, 2, \ldots, 8$. Choosing equal relaxation times leads to SRT LB schemes. This is precisely because one can choose various different relaxation times for performing collision, that one can gain numerical stability (see for instance [20] for an illustration in image processing). Following [13] and assuming $s_k \neq 0$, let denote

$$\sigma_k := \frac{1}{s_k} - \frac{1}{2}. \tag{9}$$

Computing Taylor's expansions up to the third order leads to

$$f_i + \Delta t \frac{\partial}{\partial t} f_i + \frac{\Delta t^2}{2} \frac{\partial^2}{\partial t^2} f_i + \frac{\Delta t^3}{6} \frac{\partial^3}{\partial t^3} f_i + \mathcal{O}\left(\Delta t^4\right)$$

$$
= f_i^* - \Delta t \vec{v}_i^T \cdot \vec{\nabla} f_i^* + \frac{\Delta t^2}{2} \vec{v}_i^T \cdot H\left(f_i^*\right) \cdot \vec{v}_i - \frac{\Delta t^3}{6} \vec{v}_i^T \cdot \vec{\nabla}\left(\vec{v}_i^T \cdot H\left(f_i^*\right) \cdot \vec{v}_i\right)
$$

$$
+ \Delta t F_i - \Delta t^2 \vec{v}_i^T \cdot \vec{\nabla}\left(F_i\right) + \frac{\Delta t^3}{2} \vec{v}_i^T \cdot H\left(F_i\right) \cdot \vec{v}_i + \mathcal{O}\left(\lambda^4 \Delta t^4\right), \tag{10}
$$

where H denotes the hessian bilinear form. To obtain the searched equivalent PDE, Taylor's expansions are performed in the moment space using (10). These expansions are done by assuming that the ratio $\Delta x / \Delta t$ is constant, *i.e.* at the acoustic scale, and consequently by assuming that a big $\mathcal{O}$ of $\lambda^n \Delta t^n = \Delta x^n$ is also a big $\mathcal{O}$ of Δt^n. The aim is to compute some expressions listed in Table 1, together with some components of $\vec{\mathbb{F}}$, to approximate the governing equation (1) up to a given order. Anticipating the computations detailed in the forthcoming section, Table 1 gives the expressions of the equilibrium moments that are involved regarding the governing CDE (1). As in d'Humières [8] or in Boghosian et al. [3], the equilibrium values depend only on the sole conserved moment $U\left(\vec{x}, t\right)$. Finally, these computations make use of the identity

$$
\vec{z}^T \cdot \vec{f}\left(\vec{x}, t\right) = \vec{z}^T \cdot \boldsymbol{M}^{-1} \vec{m}\left(\vec{x}, t\right). \tag{11}
$$

3. Second order equivalent PDE of a CDE

This section is devoted to the derivation of the equivalent PDE up to the second order of the MRT D2Q9 LB scheme given by (4). Note that in this section, there is no assumption on the advection velocity which can therefore be a non-constant vector field.

Proposition 1 (First order). *The equivalent PDE up to the first order of the MRT D2Q9 LB scheme* (4) *is given by*

$$
\frac{\partial}{\partial t} U\left(\vec{x}, t\right) + \lambda \vec{\nabla} \cdot \left(\vec{\alpha}_j\left(\vec{x}\right) U\left(\vec{x}, t\right)\right) = \mathbb{F}_0\left(\vec{x}, t\right) + \mathcal{O}\left(\Delta t\right). \tag{12}
$$

Remark 1. According to (1), the source term $S\left(\vec{x}, t\right)$ is given by $\mathbb{F}_0\left(\vec{x}, t\right)$. We underline the fact that the advection velocity $\vec{w}\left(\vec{x}\right)$ is given by $\lambda \vec{\alpha}_j\left(\vec{x}\right)$ and thus is rescaled by λ. Although this can be confusing, it makes the computation easier.

Proof. Equating zero order terms in (10) gives $f_i = f_i^* + \mathcal{O}\left(\Delta t\right)$. By using (6) and (8), one can easily check that

$$
m_k = m_k^* + \mathcal{O}\left(\Delta t\right) = m_k^{eq} + \mathcal{O}\left(\Delta t\right), \tag{13}
$$

$$
f_i = f_i^* + \mathcal{O}\left(\Delta t\right) = f_i^{eq} + \mathcal{O}\left(\Delta t\right). \tag{14}
$$

Dealing with the first order terms of (10), the above equations imply that

$$
m_k + \Delta t \frac{\partial}{\partial t} m_k^{eq} = m_k^* - \Delta t \sum_{i=0}^{8} M_{k,i} \vec{v}_i^T \cdot \vec{\nabla} f_i^{eq} + \Delta t \mathbb{F}_k + \mathcal{O}\left(\Delta t^2\right). \tag{15}
$$

Let us recall that $m_0 = m_0^* = m_0^{eq} = U\left(\vec{x}, t\right)$ and $M_{0,i} \vec{v}_i = \vec{v}_i$. Applying (11) to $\vec{z} = \vec{v}_x$ and $\vec{z} = \vec{v}_y$ gives

$$
\sum_{i=0}^{8} \vec{v}_i^T \cdot \vec{\nabla} f_i^{eq} = \vec{\nabla} \cdot \vec{j}^{\,eq} = \lambda \vec{\nabla} \cdot \left(\vec{\alpha}_j\left(\vec{x}\right) U\left(\vec{x}, t\right)\right). \tag{16}
$$

Replacing the above expression in (15) for $k = 0$ leads to the result. □

In the sequel, let set $\sigma_1 = \sigma_2$, *i.e.* $s_1 = s_2$, to guarantee an isotropic diffusion.

Proposition 2 (Second order). *The equivalent PDE up to the second order of the MRT D2Q9 LB scheme* (4) *is given by*

$$
\mathcal{O}\left(\Delta t^2\right) + \mathbb{F}_0\left(\vec{x}, t\right) = \frac{\partial}{\partial t} U\left(\vec{x}, t\right) + \lambda \vec{\nabla} \cdot \left(\vec{\alpha}_j\left(\vec{x}\right) U\left(\vec{x}, t\right)\right)
$$

$$
- \Delta t \lambda^2 \sigma_1 \left(\frac{\partial^2}{\partial x^2} \left(\alpha_E + \frac{1}{2} \alpha_{p_{xx}} - \alpha_{j_x}^2\left(\vec{x}\right) \right) + \frac{\partial^2}{\partial y^2} \left(\alpha_E - \frac{1}{2} \alpha_{p_{xx}} - \alpha_{j_y}^2\left(\vec{x}\right) \right) + 2 \frac{\partial^2}{\partial x \partial y} \left(\alpha_{p_{xy}} - \alpha_{j_x}\left(\vec{x}\right) \alpha_{j_y}\left(\vec{x}\right) \right) \right) U\left(\vec{x}, t\right)
$$

$$
+ A_1\left(\vec{x}, t\right) + A_2\left(\vec{x}, t\right) \tag{17}
$$

with

$$A_1\left(\vec{x}, t\right) = -\Delta t \lambda^2 \sigma_1 \vec{\nabla} \cdot \left(U\left(\vec{x}, t\right) \mathrm{J}\left(\vec{\alpha}_j\left(\vec{x}\right)\right) \cdot \vec{\alpha}_j\left(\vec{x}\right)\right), \tag{18}$$

$$A_2\left(\vec{x}, t\right) = \frac{\Delta t}{2} \frac{\partial}{\partial t} \mathbb{F}_0\left(\vec{x}, t\right) - \Delta t \lambda \sigma_1 \vec{\nabla} \cdot \left(\vec{\alpha}_j\left(\vec{x}\right) \mathbb{F}_0\left(\vec{x}, t\right)\right) + \frac{\Delta t}{s_1} \vec{\nabla} \cdot \left(\begin{array}{c} \mathbb{F}_1\left(\vec{x}, t\right) \\ \mathbb{F}_2\left(\vec{x}, t\right) \end{array}\right), \tag{19}$$

and where $\mathrm{J}\left(\vec{\alpha}_j\left(\vec{x}\right)\right)$ denotes the Jacobian of the vector $\vec{\alpha}_j\left(\vec{x}\right)$.

Remark 2. The extra terms $A_1\left(\vec{x}, t\right)$ and $A_2\left(\vec{x}, t\right)$ come from the non-constant advection velocity and the non-zero source term, respectively. The advection velocity $\vec{w}\left(\vec{x}\right)$ is given by $\lambda \vec{\alpha}_j\left(\vec{x}\right)$, the diffusion by the matrix

$$\Delta t \lambda^2 \sigma_1 \begin{pmatrix} \alpha_{\mathrm{E}} + \frac{1}{2}\alpha_{\mathrm{p}_{xx}} & \alpha_{\mathrm{p}_{xy}} \\ \alpha_{\mathrm{p}_{xy}} & \alpha_{\mathrm{E}} - \frac{1}{2}\alpha_{\mathrm{p}_{xx}} \end{pmatrix}, \tag{20}$$

and the source term $S\left(\vec{x}, t\right)$ by $\mathbb{F}_0\left(\vec{x}, t\right)$.

Proof. Equation (15) implies that

$$m_k^* - m_k = \Delta t \sum_{i=0}^{8} M_{k,i} \vec{v}_i^T \cdot \vec{\nabla} f_i^{eq} + \Delta t \frac{\partial}{\partial t} m_k^{eq} - \Delta t \mathbb{F}_k + \mathcal{O}\left(\Delta t^2\right) = s_k\left(m_k^{eq} - m_k\right). \tag{21}$$

Assuming $s_k \neq 0$ for $k = 1, 2, \ldots, 8$, this leads to

$$m_k = m_k^{eq} - \frac{\Delta t}{s_k}\left(\sum_{i=0}^{8} M_{k,i} \vec{v}_i^T \cdot \vec{\nabla} f_i^{eq} + \frac{\partial}{\partial t} m_k^{eq} - \mathbb{F}_k\right) + \mathcal{O}\left(\Delta t^2\right), \tag{22}$$

$$m_k^* = m_k^{eq} + \Delta t\left(1 - \frac{1}{s_k}\right)\left(\sum_{i=0}^{8} M_{k,i} \vec{v}_i^T \cdot \vec{\nabla} f_i^{eq} + \frac{\partial}{\partial t} m_k^{eq} - \mathbb{F}_k\right) + \mathcal{O}\left(\Delta t^2\right). \tag{23}$$

Equating second order terms in (10) gives

$$m_k + \Delta t \frac{\partial}{\partial t} m_k + \frac{\Delta t^2}{2} \frac{\partial^2}{\partial t^2} m_k^{eq} = m_k^* - \Delta t \sum_{i=0}^{8} M_{k,i} \vec{v}_i^T \cdot \vec{\nabla} f_i^* + \Delta t \mathbb{F}_k + \frac{\Delta t^2}{2} \sum_{i=0}^{8} M_{k,i} \vec{v}_i^T \cdot \mathrm{H}\left(f_i^{eq}\right) \cdot \vec{v}_i$$

$$- \Delta t^2 \sum_{i=0}^{8} M_{k,i} \vec{v}_i^T \cdot \vec{\nabla}\left(F_i\right) + \mathcal{O}\left(\Delta t^3\right). \tag{24}$$

With (16) and for $k = 0$, the above equality implies that

$$\mathcal{O}\left(\Delta t^3\right) + \Delta t \mathbb{F}_0\left(\vec{x}, t\right) = \Delta t \frac{\partial}{\partial t} U\left(\vec{x}, t\right) + \Delta t \vec{\nabla} \cdot \vec{j}^* + \Delta t^2 \vec{\nabla} \cdot \left(\begin{array}{c} \mathbb{F}_1\left(\vec{x}, t\right) \\ \mathbb{F}_2\left(\vec{x}, t\right) \end{array}\right) - \frac{\Delta t^2}{2}\left(\sum_{i=0}^{8} \vec{v}_i^T \cdot \mathrm{H}\left(f_i^{eq}\right) \cdot \vec{v}_i - \frac{\partial^2}{\partial t^2} U\left(\vec{x}, t\right)\right). \tag{25}$$

The equations (12) and (23) allow computing the divergence of $\vec{j}^*$ to obtain

$$\vec{\nabla} \cdot \vec{j}^* = \vec{\nabla} \cdot \vec{j}^{eq} + \Delta t\left(1 - \frac{1}{s_1}\right)\left(\sum_{i=0}^{8} \vec{v}_i^T \cdot \mathrm{H}\left(f_i^{eq}\right) \cdot \vec{v}_i - \frac{\partial^2}{\partial t^2} U\left(\vec{x}, t\right) + \frac{\partial}{\partial t} \mathbb{F}_0\left(\vec{x}, t\right) - \vec{\nabla} \cdot \left(\begin{array}{c} \mathbb{F}_1\left(\vec{x}, t\right) \\ \mathbb{F}_2\left(\vec{x}, t\right) \end{array}\right)\right) + \mathcal{O}\left(\Delta t^2\right). \tag{26}$$

Replacing the above expression in (25) implies that

$$\mathcal{O}\left(\Delta t^2\right) + \mathbb{F}_0\left(\vec{x}, t\right) = \frac{\partial}{\partial t} U\left(\vec{x}, t\right) + \lambda \vec{\nabla} \cdot \left(\vec{\alpha}_j\left(\vec{x}\right) U\left(\vec{x}, t\right)\right) - \Delta t \sigma_1 \left(\sum_{i=0}^{8} \vec{v}_i^T \cdot \mathrm{H}\left(f_i^{eq}\right) \cdot \vec{v}_i - \frac{\partial^2}{\partial t^2} U\left(\vec{x}, t\right)\right)$$

$$+ \Delta t\left(1 - \frac{1}{s_1}\right) \frac{\partial}{\partial t} \mathbb{F}_0\left(\vec{x}, t\right) + \frac{\Delta t}{s_1} \vec{\nabla} \cdot \left(\begin{array}{c} \mathbb{F}_1\left(\vec{x}, t\right) \\ \mathbb{F}_2\left(\vec{x}, t\right) \end{array}\right). \tag{27}$$

Now, let focus on the second order term of this last equality. The Hessian writes

$$\sum_{i=0}^{8} \vec{v}_i^T \cdot \mathrm{H}\left(f_i^{eq}\right) \cdot \vec{v}_i = \sum_{i=0}^{8}\left(v_{i,x}^2 \frac{\partial^2}{\partial x^2} + 2 v_{i,x} v_{i,y} \frac{\partial^2}{\partial x \partial y} + v_{i,y}^2 \frac{\partial^2}{\partial y^2}\right) f_i^{eq}. \tag{28}$$

Table 2

D2Q9 equilibrium of non-conserved physical moments as function of the single conserved moment U for CDE up to the second order.

Physical moment	j_x	j_y	E	p_{xx}	p_{xy}
Equilibrium	$\lambda \alpha_{j_x}(\vec{x})$	$\lambda \alpha_{j_y}(\vec{x})$	$\lambda^2 \left(\alpha_E' + \frac{\|\vec{\alpha}_j(\vec{x})\|^2}{2} \right)$	$\lambda^2 \left(\alpha_{j_x}(\vec{x})^2 - \alpha_{j_y}(\vec{x})^2 \right)$	$\lambda^2 \alpha_{j_x}(\vec{x}) \alpha_{j_y}(\vec{x})$

Equation (11) applied to $\vec{z} = \vec{v}_x \overset{H}{:} \vec{v}_x$, $\vec{z} = \vec{v}_x \overset{H}{:} \vec{v}_y$, and $\vec{z} = \vec{v}_y \overset{H}{:} \vec{v}_y$, where $\overset{H}{:}$ denotes the Hadamard product, gives

$$\sum_{i=0}^{8} \vec{v}_i^T \cdot H\left(f_i^{eq}\right) \cdot \vec{v}_i = \lambda^2 \left(\frac{\partial^2}{\partial x^2} \left(\alpha_E + \frac{1}{2} \alpha_{p_{xx}} \right) U(\vec{x}, t) + 2 \frac{\partial^2}{\partial x \partial y} \left(\alpha_{p_{xy}} U(\vec{x}, t) \right) + \frac{\partial^2}{\partial y^2} \left(\alpha_E - \frac{1}{2} \alpha_{p_{xx}} \right) U(\vec{x}, t) \right). \tag{29}$$

From (12), one obtains

$$\frac{\partial^2}{\partial t^2} U(\vec{x}, t) = -\lambda \vec{\nabla} \cdot \left(\vec{\alpha}_j(\vec{x}) \frac{\partial}{\partial t} U(\vec{x}, t) \right) + \frac{\partial}{\partial t} \mathbb{F}_0(\vec{x}, t) + \mathcal{O}(\Delta t) \tag{30}$$

$$= \lambda^2 \vec{\nabla} \cdot \left(\vec{\alpha}_j(\vec{x}) \vec{\nabla} \cdot \left(\vec{\alpha}_j(\vec{x}) U(\vec{x}, t) \right) \right) + \frac{\partial}{\partial t} \mathbb{F}_0(\vec{x}, t) - \lambda \vec{\nabla} \cdot \vec{\alpha}_j(\vec{x}) \mathbb{F}_0(\vec{x}, t)) + \mathcal{O}(\Delta t) \tag{31}$$

$$= \lambda^2 \left(\frac{\partial^2}{\partial x^2} \left(\alpha_{j_x}^2(\vec{x}) U(\vec{x}, t) \right) + 2 \frac{\partial^2}{\partial x \partial y} \left(\alpha_{j_x}(\vec{x}) \alpha_{j_y}(\vec{x}) U(\vec{x}, t) \right) + \frac{\partial^2}{\partial y^2} \left(\alpha_{j_y}^2(\vec{x}) U(\vec{x}, t) \right) \right.$$

$$\left. - \vec{\nabla} \cdot \left(U(\vec{x}, t) J(\vec{\alpha}_j(\vec{x})) \cdot \vec{\alpha}_j(\vec{x}) \right) + \frac{\partial}{\partial t} \mathbb{F}_0(\vec{x}, t) - \lambda \vec{\nabla} \cdot \left(\vec{\alpha}_j(\vec{x}) \mathbb{F}_0(\vec{x}, t) \right) + \mathcal{O}(\Delta t) \right. . \tag{32}$$

Replacing (29) and (32) in (27), leads to the result. □

In the sequel, let set

$$\alpha_E = \alpha_E' + \frac{\|\vec{\alpha}_j(\vec{x})\|^2}{2}, \quad \alpha_{p_{xx}} = \alpha_{j_x}^2(\vec{x}) - \alpha_{j_y}^2(\vec{x}), \quad \alpha_{p_{xy}} = \alpha_{j_x}(\vec{x}) \alpha_{j_y}(\vec{x}), \tag{33.a}$$

to ensure a constant and isotropic diffusion independent to the advection $\vec{\alpha}_j(\vec{x})$ and whose coefficient D is given by $\Delta t \lambda^2 \sigma_1 \alpha_E'$, where α_E' is a free parameter. Let also set

$$\mathbb{F}_1 = \left(1 - \frac{s_1}{2} \right) \lambda \alpha_{j_x}(\vec{x}) \mathbb{F}_0(\vec{x}, t), \quad \mathbb{F}_2 = \left(1 - \frac{s_1}{2} \right) \lambda \alpha_{j_y}(\vec{x}) \mathbb{F}_0(\vec{x}, t), \tag{33.b}$$

to cancel one of the additional terms arising from the non-zero source term. Consequently, we obtain the following equivalent PDE up to the second order of the MRT D2Q9 LB scheme (4):

$$\mathcal{O}\left(\Delta t^2\right) + \mathbb{F}_0(\vec{x}, t) = \frac{\partial}{\partial t} U(\vec{x}, t) + \lambda \vec{\nabla} \cdot \left(\vec{\alpha}_j(\vec{x}) U(\vec{x}, t) \right) - \Delta t \lambda^2 \alpha_E' \sigma_1 \Delta U(\vec{x}, t)$$

$$- \Delta t \lambda^2 \sigma_1 \vec{\nabla} \cdot \left(U(\vec{x}, t) J(\vec{\alpha}_j(\vec{x})) \cdot \vec{\alpha}_j(\vec{x}) \right) + \frac{\Delta t}{2} \frac{\partial}{\partial t} \mathbb{F}_0(\vec{x}, t). \tag{34}$$

Table 2 gives the equilibrium of the non-conserved moments that have to be chosen to obtain (34). The other moments, *i.e.* $\vec{q}$ and χ, and the force vector components $\mathbb{F}_k$, for $k = 3, \ldots, 8$, have no effect up to the second order in Δt.

4. Third order equivalent PDE of a CDE

This section is devoted to the derivation of the equivalent PDE up to the third order of the MRT LB scheme given by (4) when the advection velocity of the governing equation (1) is constant and the source term is null. Applying Proposition 2 in this case leads to the following:

Corollary 1 (*Second order with constant advection and no source term*). *With the setting* (33.a), (33.b) *and without forcing term, the equivalent PDE up to the second order of the MRT D2Q9 LB scheme* (4) *is given by*

$$\frac{\partial}{\partial t} U(\vec{x}, t) + \lambda \vec{\nabla} \cdot \left(\vec{\alpha}_j U(\vec{x}, t) \right) - \Delta t \lambda^2 \alpha_E' \sigma_1 \Delta U(\vec{x}, t) = \mathcal{O}\left(\Delta t^2 \right). \tag{35}$$

The proof of Proposition 3 makes use of the following lemmas.

Lemma 1. *Assuming $s_k \neq 0$, the non-conserved moments m_k for $k = 1, 2, \ldots, 8$ satisfy*

$$m_k = m_k^{eq} - \frac{\Delta t}{s_k} \left(\sum_{i=0}^{8} M_{k,i} \vec{v}_i^T \cdot \vec{\nabla} f_i^{eq} + \frac{\partial}{\partial t} m_k^{eq} - \Delta t \sigma_k \left(\frac{\partial^2}{\partial t^2} m_k^{eq} + \frac{\partial}{\partial t} \sum_{i=0}^{8} M_{k,i} \vec{v}_i^T \cdot \vec{\nabla} f_i^{eq} \right) \right.$$

$$\left. - \sum_{i=0,\ell=1}^{8} \Delta t \sigma_\ell \left(M_{i,\ell}^{-1} M_{k,i} \frac{\partial}{\partial t} \vec{v}_i^T \cdot \vec{\nabla} m_\ell^{eq} + \sum_{n=0}^{8} M_{i,\ell}^{-1} M_{k,i} M_{\ell,n} \vec{v}_i^T \cdot \mathrm{H}\left(f_n^{eq}\right) \cdot \vec{v}_n \right) \right) + \mathcal{O}\left(\Delta t^3\right) \tag{36}$$

$$m_k^* = m_k^{eq} + \Delta t \left(1 - \frac{1}{s_k} \right) \left(\sum_{i=0}^{8} M_{k,i} \vec{v}_i^T \cdot \vec{\nabla} f_i^{eq} + \frac{\partial}{\partial t} m_k^{eq} - \Delta t \sigma_k \left(\frac{\partial^2}{\partial t^2} m_k^{eq} + \frac{\partial}{\partial t} \sum_{i=0}^{8} M_{k,i} \vec{v}_i^T \cdot \vec{\nabla} f_i^{eq} \right) \right.$$

$$\left. - \sum_{i=0,\ell=1}^{8} \Delta t \sigma_\ell \left(M_{i,\ell}^{-1} M_{k,i} \frac{\partial}{\partial t} \vec{v}_i^T \cdot \vec{\nabla} m_\ell^{eq} + \sum_{n=0}^{8} M_{i,\ell}^{-1} M_{k,i} M_{\ell,n} \vec{v}_i^T \cdot \mathrm{H}\left(f_n^{eq}\right) \cdot \vec{v}_n \right) \right) + \mathcal{O}\left(\Delta t^2\right). \tag{37}$$

Proof. Equation (24), with $\frac{\partial}{\partial t} m_k$ computed from (22), gives

$$m_k^* - m_k = \Delta t \frac{\partial}{\partial t} m_k^{eq} + \Delta t \sum_{i=0}^{8} M_{k,i} \vec{v}_i^T \cdot \vec{\nabla} \left(f_i^*\right) - \frac{\Delta t^2}{s_k} \frac{\partial}{\partial t} \sum_{i=0}^{8} M_{k,i} \vec{v}_i^T \cdot \vec{\nabla} \left(f_i^{eq}\right) - \Delta t^2 \sigma_k \frac{\partial^2}{\partial t^2} m_k^{eq}$$

$$- \frac{\Delta t^2}{2} \sum_{i=0}^{8} M_{k,i} \vec{v}_i^T \cdot \mathrm{H}\left(f_i^{eq}\right) \cdot \vec{v}_i + \mathcal{O}\left(\Delta t^3\right). \tag{38}$$

Using the linear transform (6), the equality $m_0^* = m_0^{eq}$ and the equation (23) imply

$$\sum_{i=0}^{8} M_{k,i} \vec{v}_i^T \cdot \vec{\nabla} \left(f_i^*\right) = \sum_{i=0}^{8} M_{k,i} \vec{v}_i^T \cdot \vec{\nabla} \left(f_i^{eq}\right) + \Delta t \sum_{\ell=1}^{8} \left(1 - \frac{1}{s_\ell} \right) \left(\sum_{i=0}^{8} M_{i,\ell}^{-1} M_{k,i} \frac{\partial}{\partial t} \vec{v}_i^T \cdot \vec{\nabla} \left(m_\ell^{eq}\right) \right.$$

$$\left. + \sum_{n=0}^{8} M_{i,\ell}^{-1} M_{k,i} M_{\ell,n} \vec{v}_i^T \cdot \mathrm{H}\left(f_n^{eq}\right) \cdot \vec{v}_n \right) + \mathcal{O}\left(\Delta t^2\right), \tag{39}$$

which leads to the result. $\quad\square$

Lemma 2. *Given the Taylor expansions (10) with all F_i equal to zero and the MRT D2Q9 LB scheme (4), we have*

$$\mathcal{O}\left(\Delta t^3\right) = \frac{\partial}{\partial t} U\left(\vec{x}, t\right) + \vec{\nabla} \cdot \left(\vec{j}^*\right) + \frac{\Delta t}{2} \left(\frac{\partial^2}{\partial^2 t} U\left(\vec{x}, t\right) - \sum_{i=0}^{8} \vec{v}_i^T \cdot \mathrm{H}\left(f_i^*\right) \cdot \vec{v}_i \right)$$

$$+ \frac{\Delta t^2}{6} \left(\frac{\partial^3}{\partial^3 t} U\left(\vec{x}, t\right) + \sum_{i=0}^{8} \vec{v}_i^T \cdot \vec{\nabla} \left(\vec{v}_i^T \cdot \mathrm{H}\left(f_i^{eq}\right) \cdot \vec{v}_i \right) \right). \tag{40}$$

Proof. Equating terms up to the third order in (10), and using (13), leads to

$$m_k + \Delta t \frac{\partial}{\partial t} m_k + \frac{\Delta t^2}{2} \frac{\partial^2}{\partial^2 t} m_k + \frac{\Delta t^3}{6} \frac{\partial^3}{\partial^3 t} m_k^{eq} = m_k^* - \Delta t \sum_{i=0}^{8} M_{k,i} \vec{v}_i^T \cdot \vec{\nabla} \left(f_i^*\right) + \frac{\Delta t^2}{2} \sum_{i=0}^{8} M_{k,i} \vec{v}_i^T \cdot \mathrm{H}\left(f_i^*\right) \cdot \vec{v}_i$$

$$- \frac{\Delta t^3}{6} \sum_{i=0}^{8} M_{k,i} \vec{v}_i^T \cdot \vec{\nabla} \left(\vec{v}_i^T \cdot \mathrm{H}\left(f_i^{eq}\right) \cdot \vec{v}_i \right) + \mathcal{O}\left(\Delta t^4\right). \tag{41}$$

Since $m_0 = m_0^* = U$, the result follows from (16). $\quad\square$

Lemma 3. *Given the MRT D2Q9 LB scheme (4) with the setting (33.a), (33.b) and without forcing term, we have*

$$\vec{\nabla} \cdot \left(\vec{j}^*\right) = - \sum_{i=0,\ell=1}^{8} \Delta t^2 \left(1 - \frac{1}{s_1} \right) \sigma_\ell \left(\sum_{n=0}^{8} M_{\ell,i}^{-1} M_{\ell,n} \vec{v}_n^T \cdot \vec{\nabla} \left(\vec{v}_i^T \cdot \mathrm{H}\left(f_n^{eq}\right) \cdot \vec{v}_i \right) + M_{i,\ell}^{-1} \vec{v}_i^T \cdot \mathrm{H}\left(\frac{\partial}{\partial t} m_\ell^{eq} \right) \cdot \vec{v}_i \right)$$

$$+ \lambda \vec{\nabla} \cdot \left(\vec{\alpha}_j U\right) + \Delta t \lambda^2 \alpha_{\mathrm{E}}' \left(1 - \frac{1}{s_1} \right) \Delta U + \Delta t^2 \lambda^3 \alpha_{\mathrm{E}}' 2 \left(1 - \frac{1}{s_1} \right) \sigma_1 \vec{\alpha}_j^T \cdot \vec{\nabla} \left(\Delta\left(U\right) \right) + \mathcal{O}\left(\Delta t^3\right), \tag{42a}$$

$$\frac{\partial^2}{\partial^2 t} U = \lambda^2 \vec{\alpha}_j^T \cdot H(U) \cdot \vec{\alpha}_j - \Delta t \lambda^3 \alpha_{\scriptscriptstyle E}' 2\sigma_1 \vec{\alpha}_j^T \cdot \vec{\nabla}(\Delta(U)) + \mathcal{O}\left(\Delta t^2\right), \tag{42b}$$

$$\sum_{i=0}^{8} \vec{v}_i^T \cdot H\left(f_i^*\right) \cdot \vec{v}_i = \Delta t \sum_{\ell=1}^{8} \left(1 - \frac{1}{s_\ell}\right) \left(\sum_{i,n=0}^{8} M_{i,\ell}^{-1} M_{\ell,n} \vec{v}_n^T \cdot \vec{\nabla} \left(\vec{v}_i^T \cdot H\left(f_n^{eq}\right) \cdot \vec{v}_i \right) + \frac{\partial}{\partial t} M_{i,\ell}^{-1} \vec{v}_i^T \cdot H\left(m_\ell^{eq}\right) \cdot \vec{v}_i \right)$$
$$+ \lambda^2 \alpha_{\scriptscriptstyle E}' \Delta U + \lambda^2 \vec{\alpha}_j^T \cdot H(U) \cdot \vec{\alpha}_j + \mathcal{O}\left(\Delta t^2\right), \tag{42c}$$

$$\frac{\partial^3}{\partial^3 t} U = \sum_{i=0, \ell=1}^{8} \frac{\partial}{\partial t} M_{i,\ell}^{-1} \vec{v}_i^T \cdot H\left(m_\ell^{eq}\right) \cdot \vec{v}_i + \sum_{n=0}^{8} M_{i,\ell}^{-1} M_{\ell,n} \vec{v}_n^T \cdot \vec{\nabla} \left(\vec{v}_i^T \cdot H\left(f_i^{eq}\right) \cdot \vec{v}_i \right)$$
$$- \sum_{i=0}^{8} \vec{v}_i^T \cdot \vec{\nabla} \left(\vec{v}_i^T \cdot H\left(f_i^{eq}\right) \cdot \vec{v}_i \right) + \lambda^3 \alpha_{\scriptscriptstyle E}' \vec{\alpha}_j^T \cdot \vec{\nabla}(\Delta(U)) + \mathcal{O}(\Delta t). \tag{42d}$$

Proof. Equation (42a) is obtained from (37) using (35), (32) and (29). Equation (42b) follows from (37). One derives (42c) from (23) and (29). Finally, (42d) is obtained from (37) together with (29) and the equalities

$$\sum_{i=0}^{8} \vec{v}_i^T \cdot \vec{\nabla} \left(\vec{v}_i^T \cdot H\left(f_i^{eq}\right) \cdot \vec{v}_i \right) = \sum_{\substack{i,n=0 \\ \ell=1}}^{8} M_{i,\ell}^{-1} M_{\ell,n} \vec{v}_n^T \cdot \vec{\nabla} \left(\vec{v}_i^T \cdot H\left(f_i^{eq}\right) \cdot \vec{v}_i \right), \tag{43}$$

$$\frac{\partial}{\partial t} \sum_{i=0}^{8} \vec{v}_i^T \cdot H\left(f_i^{eq}\right) \cdot \vec{v}_i = \frac{\partial}{\partial t} \sum_{i=0, \ell=1}^{8} M_{i,\ell}^{-1} \vec{v}_i^T \cdot H\left(m_\ell^{eq}\right) \cdot \vec{v}_i. \quad \square \tag{44}$$

Proposition 3 *(Third order with constant advection and no source term). With the setting* (33.a)*,* (33.b) *and without forcing term, the equivalent PDE up to the third order of the MRT D2Q9 LB scheme* (4) *is given by*

$$\mathcal{O}\left(\Delta t^3\right) = \frac{\partial}{\partial t} U(\vec{x}, t) + \lambda \vec{\nabla} \cdot (\vec{\alpha}_j U(\vec{x}, t)) - \Delta t \lambda^2 \alpha_{\scriptscriptstyle E}' \sigma_1 \Delta U(\vec{x}, t) - \Delta t^2 \lambda^3 \alpha_{\scriptscriptstyle E}' 2 \left(\sigma_1^2 - \frac{1}{12}\right) \vec{\alpha}_j^T \cdot \vec{\nabla}(\Delta(U))$$

$$+ \Delta t^2 \lambda^3 \left(\sigma_1 \sigma_3 - \frac{1}{12}\right) \vec{\alpha}_j \overset{\scriptscriptstyle H}{:} \left(\vec{\alpha}_q - \alpha_{\scriptscriptstyle E}' \frac{\|\vec{\alpha}_j\|^2}{2}\right)^T \cdot \vec{\nabla}(\Delta(U))$$

$$+ \Delta t^2 \lambda^3 \left(\sigma_1 \sigma_4 - \frac{1}{12}\right) \vec{\alpha}_j \overset{\scriptscriptstyle H}{:} \begin{pmatrix} \frac{1}{2}\left(\alpha_{j_y}^2 - \alpha_{j_x}^2\right) + 1 - \alpha_{q_x} \\ \frac{1}{2}\left(\alpha_{j_y}^2 - \alpha_{j_x}^2\right) - 1 + \alpha_{q_y} \end{pmatrix}^T \cdot \vec{\nabla} \left(\frac{\partial^2}{\partial x^2} - \frac{\partial^2}{\partial y^2}\right) U$$

$$+ 2\Delta t^2 \lambda^3 \left(\sigma_1 \sigma_5 - \frac{1}{12}\right) \begin{pmatrix} \alpha_{j_y}\left(2\alpha_{q_y} - 1 - \alpha_{j_x}^2\right) \\ \alpha_{j_x}\left(2\alpha_{q_x} - 1 - \alpha_{j_y}^2\right) \end{pmatrix}^T \cdot \vec{\nabla} \left(\frac{\partial^2}{\partial x \partial y} U\right). \tag{45}$$

Proof. Inserting (42) in (40) leads to

$$\mathcal{O}\left(\Delta t^3\right) = \Delta t^2 \sum_{\ell=1}^{8} \left(\sigma_1 \sigma_\ell - \frac{1}{12}\right) \left(\sum_{i=0}^{8} \frac{\partial}{\partial t} M_{i,\ell}^{-1} \vec{v}_i^T \cdot H\left(m_\ell^{eq}\right) \cdot \vec{v}_i + \sum_{n=0}^{8} M_{i,\ell}^{-1} M_{\ell,n} \vec{v}_n^T \cdot \vec{\nabla} \left(\vec{v}_i^T \cdot H\left(f_n^{eq}\right) \cdot \vec{v}_i \right) \right)$$

$$+ \frac{\partial}{\partial t} U + \lambda \vec{\nabla} \cdot (\vec{\alpha}_j U) - \Delta t \lambda^2 \alpha_{\scriptscriptstyle E}' \sigma_1 \Delta U - \Delta t^2 \lambda^3 \alpha_{\scriptscriptstyle E}' 2 \left(\sigma_1^2 - \frac{1}{12}\right) \vec{\alpha}_j^T \cdot \vec{\nabla}(\Delta(U)). \tag{46}$$

One can check from (11) that

$$\sum_{i=0}^{8} M_{i,\ell}^{-1} \vec{v}_i^T \cdot H(\#) \cdot \vec{v}_i = \sum_{i=0}^{8} M_{i,\ell}^{-1} \left(v_{i,x}^2 \frac{\partial^2}{\partial^2 x} + 2 v_{i,x} v_{i,y} \frac{\partial^2}{\partial x \partial y} + v_{i,y}^2 \frac{\partial^2}{\partial^2 y} \right)(\#)$$

$$= \sum_{i=0}^{8} M_{i,\ell}^{-1} \left(\left(\frac{M_{3,i} + 4\lambda^2 M_{0,i}}{6} + \frac{1}{2} M_{4,i}\right) \frac{\partial^2}{\partial^2 x} + 2 M_{5,i} \frac{\partial^2}{\partial x \partial y} + \left(\frac{M_{3,i} + 4\lambda^2 M_{0,i}}{6} - \frac{1}{2} M_{4,i}\right) \frac{\partial^2}{\partial^2 y} \right)(\#) \tag{47}$$

$$= \frac{1}{6} \delta_3^\ell \left(\frac{\partial^2}{\partial^2 x} + \frac{\partial^2}{\partial^2 y}\right)(\#) + \frac{2}{3} \lambda^2 \delta_0^\ell \left(\frac{\partial^2}{\partial^2 x} + \frac{\partial^2}{\partial^2 y}\right)(\#) + \frac{1}{2} \delta_4^\ell \left(\frac{\partial^2}{\partial^2 x} - \frac{\partial^2}{\partial^2 y}\right)(\#) + 2\delta_5^\ell \frac{\partial^2}{\partial x \partial y}(\#) \tag{48}$$

where δ_i^n denotes the Kronecker symbol. Consequently, only the indices $\ell = 3, 4, 5$ have to be considered in (46).

For $\ell = 3$, equation (11) applied to the x and y-components of $\left(\frac{\|\vec{v}_n\|^2}{2} - \frac{2\lambda^2}{3} \right) \vec{v}_n$ gives

$$\sum_{i=0}^{8} \frac{\partial}{\partial t} M_{i,3}^{-1} \vec{v}_i^T \cdot H\left(m_3^{eq}\right) \cdot \vec{v}_i + \sum_{n=0}^{8} M_{i,3}^{-1} M_{3,n} \vec{v}_n^T \cdot \vec{\nabla}\left(\vec{v}_i^T \cdot H\left(f_n^{eq}\right) \cdot \vec{v}_i \right) = \lambda^3 \vec{\alpha}_j \cdot^{H} \left(\vec{\alpha}_q - \alpha'_E - \frac{\|\vec{\alpha}_j\|^2}{2} \right)^T \cdot \vec{\nabla}\left(\Delta\left(U\right) \right). \quad (49)$$

In the same way, with the x and y-components of $\vec{v}_n \left(v_{n,x}^2 - v_{n,y}^2 \right)/2$, for $\ell = 4$, one gets

$$\sum_{i=0}^{8} \frac{\partial}{\partial t} M_{i,4}^{-1} \vec{v}_i^T \cdot H\left(m_4^{eq}\right) \cdot \vec{v}_i + \sum_{n=0}^{8} M_{i,4}^{-1} M_{4,n} \vec{v}_n^T \cdot \vec{\nabla}\left(\vec{v}_i^T \cdot H\left(f_n^{eq}\right) \cdot \vec{v}_i \right)$$

$$= \lambda^3 \vec{\alpha}_j \cdot^{H} \begin{pmatrix} \frac{1}{2}\left(\alpha_{j_y}^2 - \alpha_{j_x}^2\right) + 1 - \alpha_{q_x} \\ \frac{1}{2}\left(\alpha_{j_y}^2 - \alpha_{j_x}^2\right) - 1 + \alpha_{q_y} \end{pmatrix}^T \cdot \vec{\nabla}\left(\frac{\partial^2}{\partial x^2} - \frac{\partial^2}{\partial y^2} \right) U.$$

Finally, with x and y-components of $2 v_{n,x} v_{n,y} \vec{v}_n$, for $\ell = 5$, one gets

$$\sum_{i=0}^{8} \frac{\partial}{\partial t} M_{i,5}^{-1} \vec{v}_i^T \cdot H\left(m_5^{eq}\right) \cdot \vec{v}_i + \sum_{n=0}^{8} M_{i,5}^{-1} M_{5,n} \vec{v}_n^T \cdot \vec{\nabla}\left(\vec{v}_i^T \cdot H\left(f_n^{eq}\right) \cdot \vec{v}_i \right) = 2\lambda^3 \begin{pmatrix} \alpha_{j_y}\left(2\alpha_{q_y} - 1 - \alpha_{j_x}^2\right) \\ \alpha_{j_x}\left(2\alpha_{q_x} - 1 - \alpha_{j_y}^2\right) \end{pmatrix}^T \cdot \vec{\nabla}\left(\frac{\partial^2}{\partial x \partial y} U \right).$$

$$(50)$$

Inserting these three expressions in (46) gives the result. $\square$

In consequence, we have the following

Corollary 2. *With the setting* (33.a), (33.b), *without forcing term, and by setting*

$$\sigma_1 = \sigma_2 = \sigma_3 = \sigma_4 = \sigma_5 = \frac{1}{\sqrt{12}}, \tag{51}$$

the equivalent PDE up to the third order of the MRT D2Q9 LB scheme (4) *is given by*

$$\mathcal{O}\left(\Delta t^3\right) = \frac{\partial}{\partial t} U\left(\vec{x}, t\right) + \lambda \vec{\nabla} \cdot \left(\vec{\alpha}_j U\left(\vec{x}, t\right)\right) - \frac{\Delta t \lambda^2 \alpha'_E}{\sqrt{12}} \Delta U\left(\vec{x}, t\right). \tag{52}$$

This means precisely that, with the conditions (33.a) and (33.b) fulfilled, the condition (51) allows increasing the accuracy of the MRT LB scheme (4) regarding the governing equation (1) and under stability conditions (see Section 4.1). The constant advection velocity $\vec{w}$ is given by $\lambda \vec{\alpha}_j$ and the diffusion coefficient D is given by $\frac{\Delta t \lambda^2 \alpha'_E}{\sqrt{12}}$.

Remark 3. Contrary to a SRT LB scheme, the relaxation times s_6, s_7 and s_8 of the MRT LB schemes used in Corollary 2 remain free. As discussed below (see also Fig. 3), they are tuned to improve numerical stability.

4.1. Von Neumann analysis: the scheme stability region

As Lallemand and Luo [15] or Servan-Camas and Tsai [21], the stability of the MRT D2Q9 LB scheme of Corollary 2 is studied from the classical Von Neumann analysis in the Fourier space. Let

$$\vec{f}\left(\vec{x}, t\right) = \vec{f}^0\left(\vec{x}, t\right) + \delta \vec{f}\left(\vec{x}, t\right), \tag{53}$$

where $\delta \vec{f}$ is a small fluctuation and $\vec{f}^0$ the uniform equilibrium state specified by the unique conserved moment U. In Fourier space, inserting (53) in the discretized Boltzmann's equation (4) without forcing term leads to

$$\delta \vec{f}(\vec{x}, t + \Delta t) = \text{diag}\left(e^{\imath \Delta t \vec{k}^T \cdot \vec{v}_i} \right) M^{-1} C M \, \delta \vec{f}\left(\vec{x}, t\right) = G \, \delta \vec{f}\left(\vec{x}, t\right), \tag{54}$$

where $\vec{k}$ is a wave vector, C the matrix of the collision operator in the moment space, and G the so-called amplification matrix:
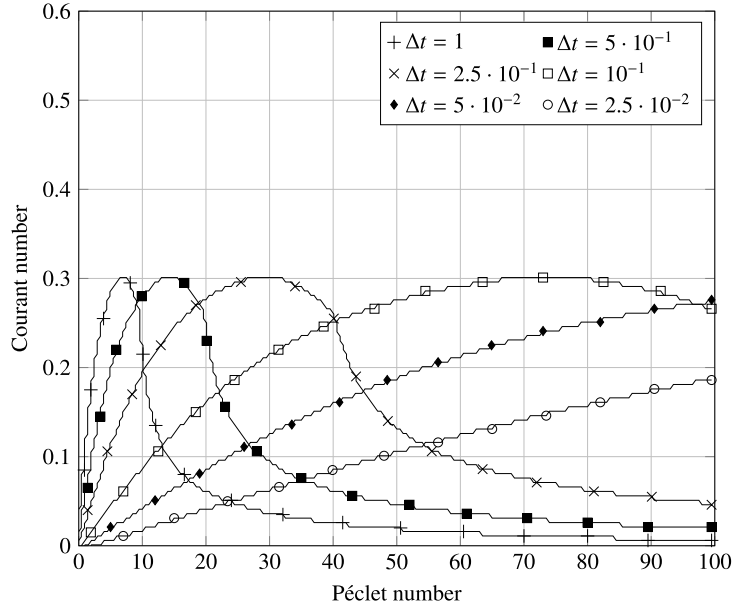
Fig. 2. Numerical stability region as a function of the Courant and Péclet number. Each plot represents the upper bound to have a scheme stable for $\lambda = 1$, $\theta = \frac{\pi}{4}$, $s_6 = s_7 = s_8 = 1.1$, and different given values of Δt. The wave vector $\vec{k}$ is discretized as $\vec{k}_{a,b} = \left\| \pi \frac{a}{30} \right\| \left(\cos\left(\pi \frac{b}{30} \right), \sin\left(\pi \frac{b}{30} \right) \right)$ with $a, b = 0, 1, \ldots, 30$.

$$G = \operatorname{diag}\left(e^{\imath \Delta t \vec{k}^T \cdot \vec{v}_i} \right) M^{-1} C M. \tag{55}$$

Let us write the advection velocity $\vec{w} = \|\vec{w}\| (\cos\theta, \sin\theta)$. Let Cr and Pe be the Courant and Péclet number defined by

$$\mathrm{Cr} = \frac{\|\vec{w}\|}{\lambda}, \quad \mathrm{Pe} = \frac{\|\vec{w}\| x_c}{D}, \tag{56}$$

where x_c is the characteristic length. From (8), by setting $x_c = 1, \alpha_{q_x} = \alpha_{q_y} = \alpha_\chi = 0$, $s_6 = s_7 = s_8$, and using the setting (33.a), (33.b), and (51), the matrix C of (54) writes

$$C = \begin{pmatrix} 1 & 0 & 0 & 0 & 0 & 0 & 0 & 0 & 0 \\ \lambda\left(3 - \sqrt{3}\right) \mathrm{Cr}\cos\theta & \sqrt{3} - 2 & 0 & 0 & 0 & 0 & 0 & 0 & 0 \\ \lambda\left(3 - \sqrt{3}\right) \mathrm{Cr}\sin\theta & 0 & \sqrt{3} - 2 & 0 & 0 & 0 & 0 & 0 & 0 \\ \lambda^2\left(3 - \sqrt{3}\right)\left(6\mathrm{Cr}\left(\frac{\sqrt{12}}{\mathrm{Pe}\lambda\Delta t} + \frac{\mathrm{Cr}}{2}\right) - 4\right) & 0 & 0 & \sqrt{3} - 2 & 0 & 0 & 0 & 0 & 0 \\ \lambda^2\left(3 - \sqrt{3}\right) \mathrm{Cr}^2\cos(2\theta) & 0 & 0 & 0 & \sqrt{3} - 2 & 0 & 0 & 0 & 0 \\ \lambda^2\left(3 - \sqrt{3}\right) \mathrm{Cr}^2\frac{1}{2}\sin(2\theta) & 0 & 0 & 0 & 0 & \sqrt{3} - 2 & 0 & 0 & 0 \\ \lambda^3 s_6\left(-5\mathrm{Cr}\cos\theta\right) & 0 & 0 & 0 & 0 & 0 & 1 - s_6 & 0 & 0 \\ \lambda^3 s_6\left(-5\mathrm{Cr}\sin\theta\right) & 0 & 0 & 0 & 0 & 0 & 0 & 1 - s_6 & 0 \\ \lambda^4 s_6\left(4 - 21\mathrm{Cr}\left(\frac{\sqrt{12}}{\mathrm{Pe}\lambda\Delta t} + \frac{\mathrm{Cr}}{2}\right)\right) & 0 & 0 & 0 & 0 & 0 & 0 & 0 & 1 - s_6 \end{pmatrix}, \tag{57}$$

and depends on $\lambda, \mathrm{Cr}, \theta, \mathrm{Pe}, \Delta t$ and s_6.

Using (54), the stability of the scheme is equivalent to an eigenvalue problem. These eigenvalues, denoted z_i for $i = 0, 1, \ldots, 8$, are solutions of the dispersion equation

$$\det\left(G - z Id \right) = 0. \tag{58}$$

The scheme is stable as long as $|z_i| \leq 1$ for $i = 0, 1, \ldots, 8$ and for all wave vector $\vec{k}$. Therefore, the stability of the scheme depends on Cr, θ, Pe, λ, Δt and s_6. Fig. 2, resp. Fig. 3 shows the stability region for different given values of Δt, resp. of s_6, and for Cr varying in $[0; 1]$ and Pe varying in $]0; 100]$.
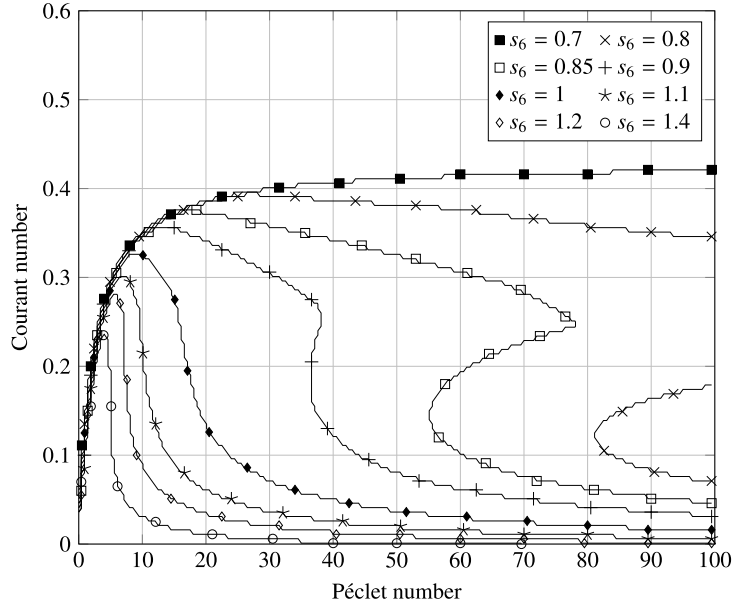
Fig. 3. Numerical stability region as a function of the Courant and Péclet number. Each plot represents the upper bound to have a scheme stable for $\lambda = 1$, $\theta = \frac{\pi}{4}$, $\Delta t = 1$, and different given values of $s_6 = s_7 = s_8$. The wave vector $\vec{k}$ is discretized as $\vec{k}_{a,b} = \left\| \pi \frac{a}{30} \right\| \left(\cos \left(\pi \frac{b}{30} \right), \sin \left(\pi \frac{b}{30} \right) \right)$ with $a, b = 0, 1, \ldots, 30$.

4.2. Numerical validation

In the sequel, we validate numerically the accuracy of the MRT D2Q9 LB scheme of Corollary 2 for Pe and Cr within the stability region provided in Fig. 2 and 3. Let us consider the governing equation (1) with constant advection $\vec{w}$ and without source term on the domain $\Omega = [0; 1]^2$ with periodic boundary conditions and initial condition given by

$$U(\vec{x}, 0) = \sqrt{2\pi} \exp \left(-\frac{\left(x - \frac{1}{2} \right)^2 + \left(y - \frac{1}{2} \right)^2}{2\varpi^2} \right), \quad \forall \vec{x} \in \Omega, \tag{59}$$

where ϖ is equal to $3 \cdot 10^{-2}$. The analytical solution of this problem writes

$$U^{\text{TH}} (\vec{x}, t) = \frac{\varpi^2 \sqrt{2\pi}}{2Dt + \varpi^2} \exp \left(-\frac{\left(x - \frac{1}{2} - w_x t \right)^2 + \left(y - \frac{1}{2} - w_y t \right)^2}{4Dt + 2\varpi^2} \right), \quad \forall (\vec{x}, t) \in \Omega \times \mathbb{R}^+. \tag{60}$$

This solution was simulated using the MRT D2Q9 LB scheme of Corollary 2 where $\vec{w} = \lambda \vec{\alpha}_j$ and $D = \frac{\Delta t \lambda^2 \alpha'_{\text{E}}}{\sqrt{12}}$. The parameters of the MRT LB scheme were set to

$$\lambda = 1, \ \Delta t = \frac{\Delta x}{\lambda}, \ \alpha_{q_x} = \alpha_{q_y} = \alpha_\chi = 0, \text{ and } s_6 = s_7 = s_8 = \frac{1}{2}. \tag{61}$$

The advection velocity was chosen equal to $\vec{w} = 2.5 \cdot 10^{-3} \times \left(\cos \left(\frac{\pi}{4} \right), \sin \left(\frac{\pi}{4} \right) \right)$ and the diffusion coefficient equal to $D = 6.25 \cdot 10^{-4}$. This choice of $\vec{w}$ and D is equivalent to Cr $= 2.5 \cdot 10^{-3}$ and Pe $= 4$. The convergence was investigated by letting Δt varies as follows:

$$\Delta t = \frac{1}{\ell \cdot 20}, \ \ell = 5, 6, \ldots, 23. \tag{62}$$

When Δt varies, the diffusion coefficient of the equivalent PDE is kept constant by setting α'_{E} equal to $\frac{D\sqrt{12}}{\Delta t \lambda^2}$. The relative error

$$Err \left(U^{\text{LB}} - U^{\text{TH}} \right) = \frac{\sqrt{\sum_{\vec{x} \in \mathcal{L}} \left(U^{\text{LB}} (\vec{x}) - U^{\text{TH}} (\vec{x}) \right)^2}}{\sqrt{\sum_{\vec{x} \in \mathcal{L}} U^{\text{TH}} (\vec{x})^2}}, \tag{63}$$
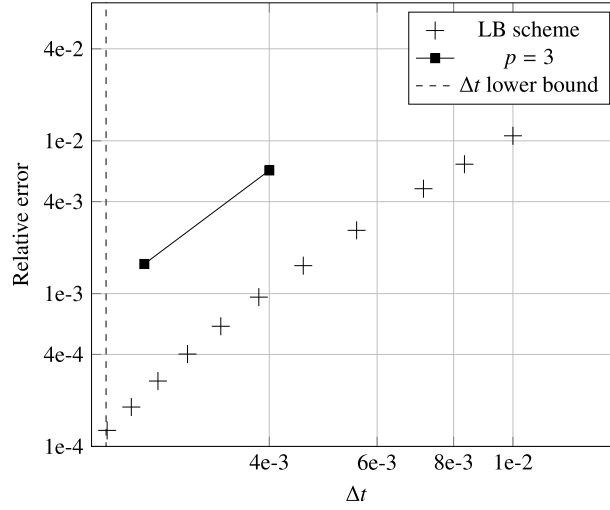
Fig. 4. Convergence curve of the simulated solution using the third order MRT LB scheme. The lower bound of Δt is given by (64). See text for details.

between the simulated solution U^{LB} and the analytical solution U^{TH} was computed for each space step after $\frac{t_f}{\Delta t}$ temporal iterations where $t_f = 5 \cdot 10^{-2}$ is the final time. According to Lallemand and Luo [15] and to Boghosian et al. [3], the condition $\alpha'_{\mathrm{E}} \in]0; 1[$ has to be satisfied to avoid instability. This condition gives the domain of validity of the expansion (52) of Corollary 2 because

$$\alpha'_{\mathrm{E}} < 1 \Longleftrightarrow \Delta t > \frac{D\sqrt{12}}{\lambda^2}. \tag{64}$$

In this simulation, $D = 6.25 \cdot 10^{-4}$ and $\lambda = 1$. Therefore, the lower bound of Δt is equal to $2.165 \cdot 10^{-3}$. Finally, the so-obtained convergence curve of the MRT D2Q9 LB scheme is a straight line with slope $p \simeq 3$ (see Fig. 4).

5. MRT LB schemes of CDE for marine radar image processing

The main topic of this section is to exploit the MRT LB schemes previously described to perform radar image processing. This is in fact what motivated us for studying such schemes.

5.1. Context and methodology

The images to be processed are RDM that allow to visualize radar signals in the frequency domain. These images are highly corrupted by an interference noise, have low contrast, and the objects to be detected have no apparent contours. Figs. 5a and 7a show a RDM image obtained from two different acquisitions provided by the CSIR small boat trails sea clutter database. The processing aims to figure out two kinds of information. The first one is relative to the sea clutter and the second one to the potential presence of objects of interest, *e.g.* targets.

To better detect these objects of interest, a first processing is performed to remove as much as possible sea clutter. This has been the subject of a previous contribution [18]. Let us just mention here that the proposed algorithm makes use of a Chan-Vese k-phase diffuse interface motion PDE. Figs. 5b and 7b show the result obtained after applying this processing on the original RDM image.

It appears that this resulting image still contains noise due to the sea clutter and that the object of interest is still difficult to identify (see Figs. 5b and 7b). To improve the processing, the resulting image is considered as the initial condition $U(\vec{x}, 0)$ of a CDE. The diffusion aims to remove the remaining noise, and the advection to enhance the signal of interest. The advection velocity $\vec{w}(\vec{x})$ is the gradient $\vec{\nabla} U(\vec{x}, 0)$ of the resulting image (obtained numerically from Figs. 5b and 7b), and the reaction-diffusion is given by the Allen-Cahn equation [1]. Therefore, the governing equation to be simulated writes

$$\frac{\partial}{\partial t} U(\vec{x}, t) + \vec{\nabla} \cdot (\vec{w}(\vec{x}) U(\vec{x}, t)) - \varepsilon \frac{\mu}{c_W} \Delta U(\vec{x}, t) = -\frac{\mu}{\varepsilon c_W} W'(U), \tag{65}$$

where μ is a regularization coefficient, ε is the width of the diffuse interface, and W is the double-well potential defined by $W(x) = x^2 (1-x)^2 / 2$. The constant c_W is given by

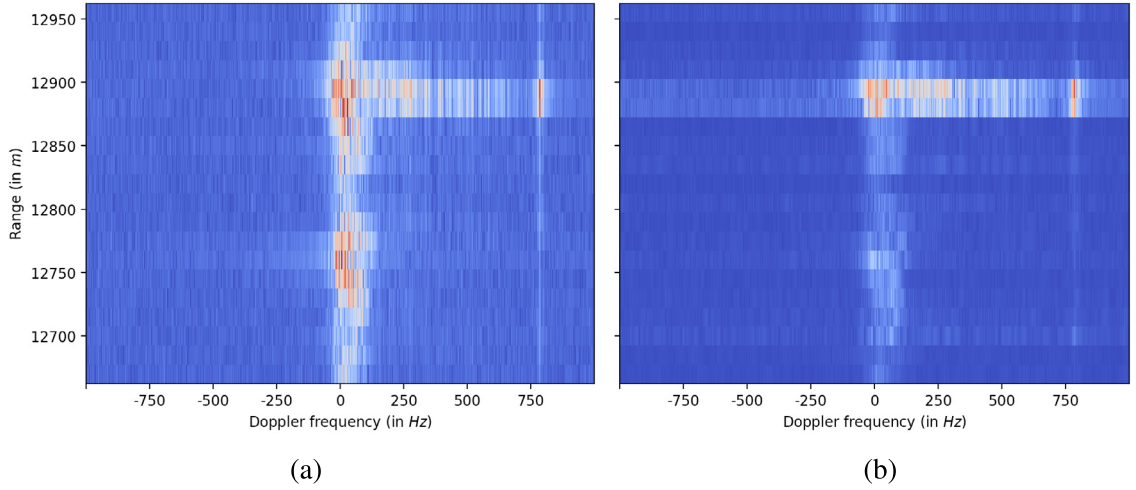$$c_W = \int_0^1 W(x)\,\mathrm{d}x \simeq \frac{1}{60}. \tag{66}$$

Fig. 5. Marine radar RDM image processing. (a): Original RDM image – (b): RDM image after sea clutter removal using [18]. Note that the scale is the same for all images.

Due to the frequency nature of the x-coordinate, periodic boundary conditions are imposed on the left and right boundaries, whereas homogeneous Neumann conditions are imposed on the upper and lower boundaries.

5.2. Experiments

The governing equation (65) is simulated using the MRT D2Q9 LB scheme (4) with the setting (33.a), (33.b) and (51). In the equivalent PDE (34) of the used LB scheme, the advection velocity $\vec{w}(\vec{x})$ is equal to $\lambda\vec{\alpha}_j(\vec{x})$, the diffusion coefficient $\varepsilon\mu/c_W$ to $\Delta t\lambda^2\alpha'_{\mathrm{E}}/\sqrt{12}$ and the force term $\mathbb{F}_0(\vec{x},t)$ to $-W'(U)\mu/(\varepsilon c_W)$. For a given threshold tol, the stopping criterion of the algorithm is

$$\frac{\left\|U(\vec{x}, t+\Delta t) - U(\vec{x},t)\right\|_{L^2}}{\left\|U(\vec{x}, t+\Delta t)\right\|_{L^2}} \le \text{tol}. \tag{67}$$

The remaining set of parameters for the simulation is given by $\lambda = 10$, $\Delta x = 1$, $\Delta t = \Delta x/\lambda$, tol $= 10^{-4}$, $\alpha_{q_x} = \alpha_{q_y} = \alpha_\chi = 0$, and $s_6 = s_7 = s_8 = 1$. Nondimensionalizing this scheme leads to consider the following parameters:

$$\vec{\alpha}_j(\vec{x}) \leftarrow \vec{\alpha}_j(\vec{x}) \overset{\text{H}}{\because} \begin{pmatrix} 1/x_c \\ 1/y_c \end{pmatrix}, \quad \alpha_{\mathrm{E}} = \lambda^2\left(\frac{\alpha'_{\mathrm{E}}}{2}\left(\frac{1}{x_c^2} + \frac{1}{y_c^2}\right) + \frac{\left\|\vec{\alpha}_j(\vec{x})\right\|^2}{2}\right),$$

$$\text{and } \alpha_{\mathrm{p}_{xx}} = \lambda^2\left(\left(\alpha^2_{j_x}(\vec{x}) - \alpha^2_{j_y}(\vec{x})\right) + \alpha'_{\mathrm{E}}\left(\frac{1}{x_c^2} - \frac{1}{y_c^2}\right)\right), \tag{68}$$

where x_c and y_c denote the characteristic units of the x and y variables, respectively. For the data in Figs. 5a and 7a, the value of x_c is equal to 3.125 Hz and y_c to 15 m. Therefore, nondimensionalizing this scheme leads to consider an anisotropic diffusion.

Remark 4. The chosen relaxation times are those that ensure the third order accuracy when the advection velocity is constant and without source term (see Proposition 3). This choice is motivated by the following observation: as shown in Fig. 8, the extra term $A_1(\vec{x},t)$ due to non-constant advection velocity becomes negligible during the iterations when compared to the advection and diffusion terms.

The result of the entire processing is shown in Fig. 6 for different values of ε and μ. With the same value of λ, it helps understand the behavior of the solution only as a function of ε and μ. For $\mu = 10^{-2}$ and $\varepsilon = 5 \cdot 10^{-2}$, all the remaining noise has been removed and the object of interest, *i.e.* the target and the waves from its wake, are now clearly isolated (see Figs. 6a and 7c).

5.3. SRT versus MRT stability

As mentioned in the introduction, applications of LB methods to image processing require to deal with MRT LB schemes, instead of SRT LB schemes. This is particularly the case when the images to be processed are highly corrupted by noise and
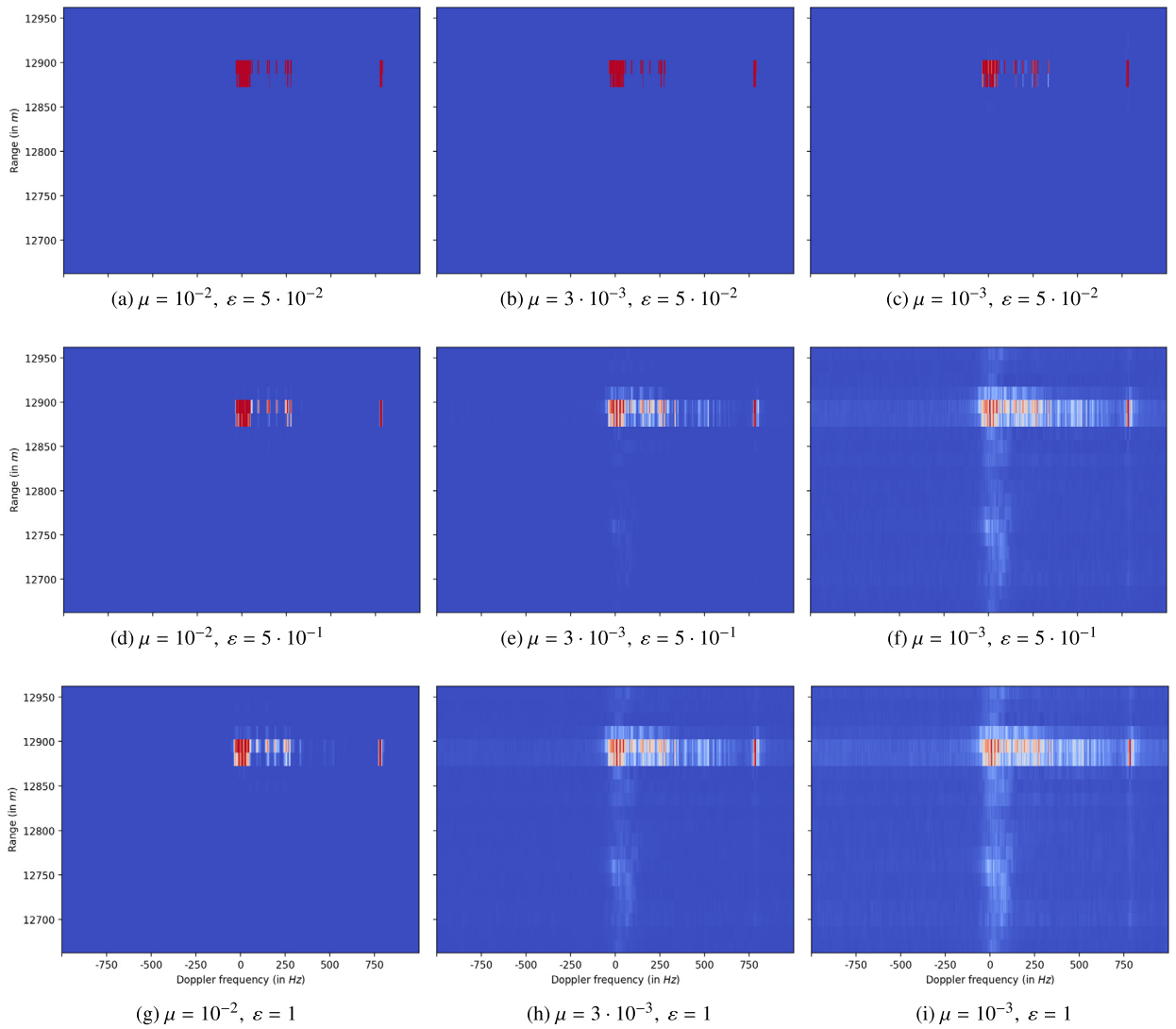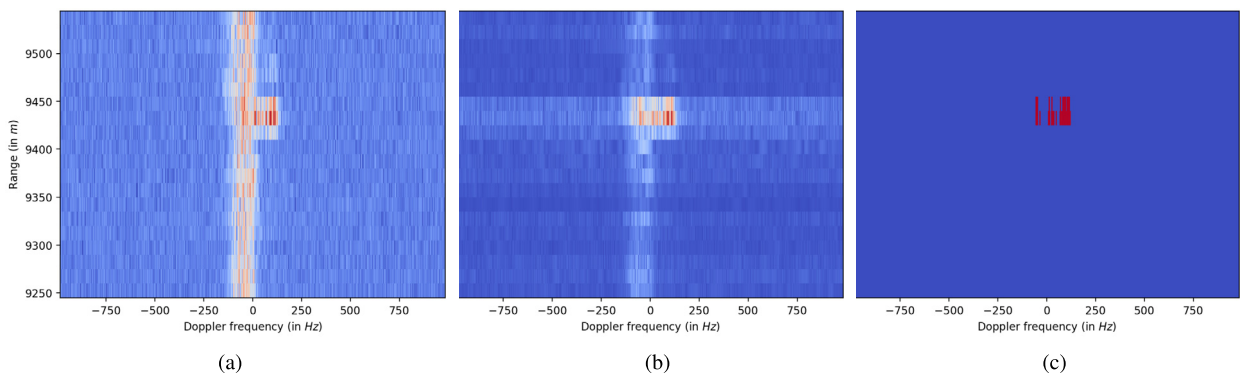
(a) $\mu = 10^{-2}$, $\varepsilon = 5 \cdot 10^{-2}$

(b) $\mu = 3 \cdot 10^{-3}$, $\varepsilon = 5 \cdot 10^{-2}$

(c) $\mu = 10^{-3}$, $\varepsilon = 5 \cdot 10^{-2}$

(d) $\mu = 10^{-2}$, $\varepsilon = 5 \cdot 10^{-1}$

(e) $\mu = 3 \cdot 10^{-3}$, $\varepsilon = 5 \cdot 10^{-1}$

(f) $\mu = 10^{-3}$, $\varepsilon = 5 \cdot 10^{-1}$

(g) $\mu = 10^{-2}$, $\varepsilon = 1$

(h) $\mu = 3 \cdot 10^{-3}$, $\varepsilon = 1$

(i) $\mu = 10^{-3}$, $\varepsilon = 1$

Fig. 6. RDM image obtained from 5b with the MRT D2Q9 LB scheme for CDE using (33.a), (33.b), and (51). Each row corresponds to a given value of ε while each column corresponds to a given value of μ. Note that the scale is the same for all images.

(a)

(b)

(c)

Fig. 7. Marine radar RDM image processing. (a): Original RDM image – (b): RDM image after sea clutter removal using [18] – (c): RDM image obtained from 7b with the MRT D2Q9 LB scheme for CDE defined by the setting (33.a), (33.b), and (51) and where μ is equal to 10^{-2} and ε to $5 \cdot 10^{-2}$. Note that the scale is the same for all images.

(a) Advection term.

(b) Diffusion term.

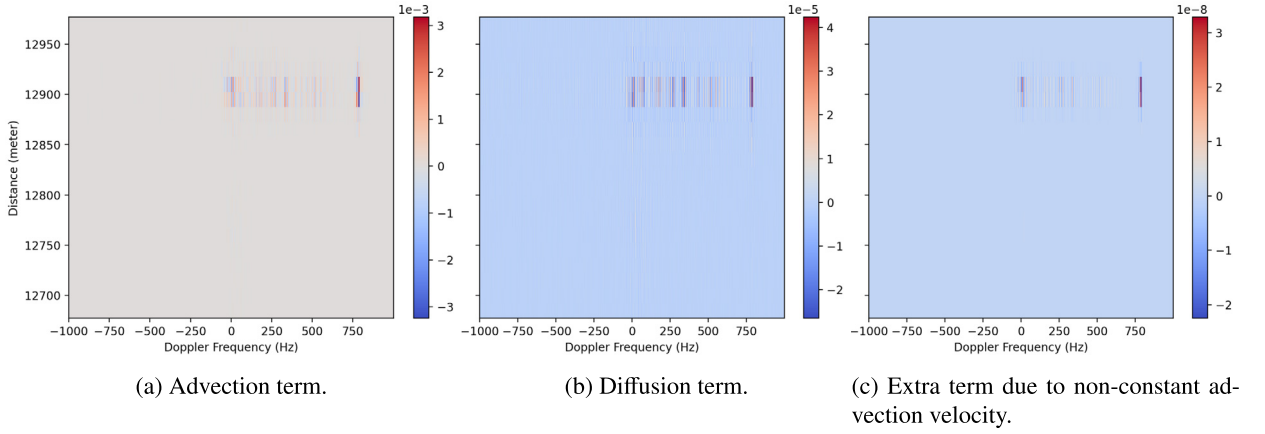(c) Extra term due to non-constant advection velocity.

Fig. 8. The extra term $A_1(\vec{x}, t)$ of Proposition 2 due to non-constant advection velocity is negligible when compared to the advection and diffusion terms.
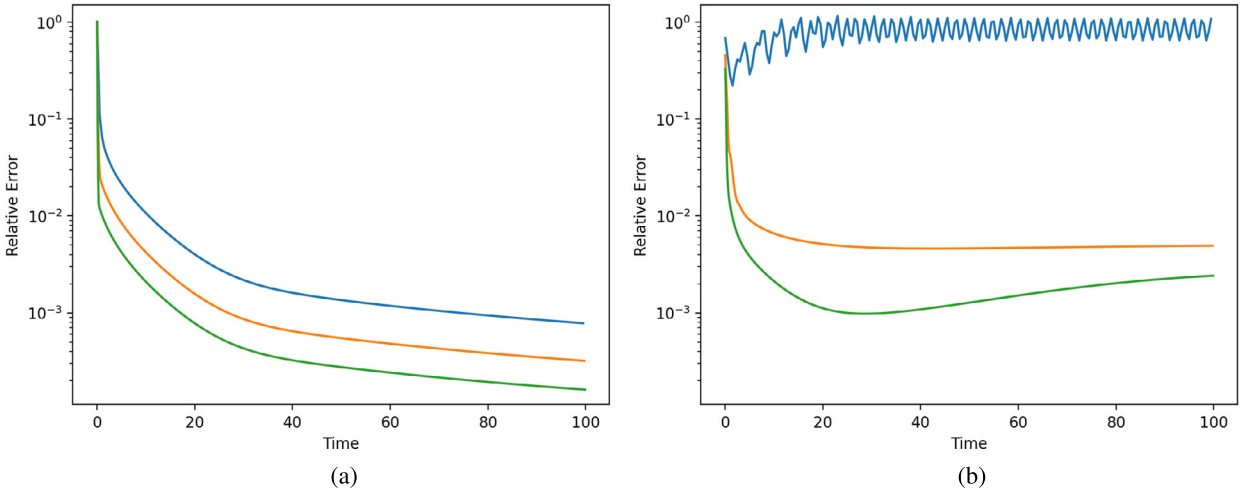

Fig. 9. Relative error in (67) for different time steps Δt. (a) MRT LB scheme and (b) SRT LB scheme. The blue, orange and green line are obtained with Δt equal to $0.5, 0.2$ and 0.1 respectively. Note that the scale is the same to ease the convergence comparison between the MRT and SRT LB schemes. (For interpretation of the colors in the figure(s), the reader is referred to the web version of this article.)

with non-apparent contours. As in [19,20], an illustration of the lack of stability when using a SRT LB sheme is given in this subsection, whereas the use of a well-chosen MRT LB scheme ensures stability.

The governing equation is given by (1) with a non-constant advection velocity $\vec{w} = \vec{\nabla} U(\vec{x}, 0)$ computed from Fig. 7b, a diffusion coefficient D equal to $6 \cdot 10^{-2}$, and $S(\vec{x}, t) = 0$, i.e. without source term. The initial and boundary conditions are the same as in Subsection 5.2. The parameters of the MRT LB scheme are set to

$$\lambda \vec{\alpha}_j = \vec{w}(\vec{x}), \ \vec{\mathbb{F}} = \vec{0}, \ \alpha_E = \alpha'_E + \frac{\|\vec{\alpha}_j\|^2}{2}, \ \alpha'_E = \frac{D}{\Delta t \lambda^2 \sigma_1}, \ \alpha_{p_{xx}} = \alpha_{j_x}^2 - \alpha_{j_y}^2, \ \alpha_{p_{xy}} = \alpha_{j_x} \alpha_{j_y},$$

$$\Delta x = 1, \ \sigma_1 = \sigma_2 = \sigma_3 = \sigma_4 = \sigma_5 = \frac{1}{\sqrt{12}}, \ s_6 = s_7 = s_8 = 1, \ \alpha_{q_x} = \alpha_{q_y} = \alpha_\chi = 0. \quad (69)$$

The unique relaxation time of the SRT LB scheme is fixed to $s = 1/2 + 3D/(\Delta t \lambda^2)$ and its equilibrium distribution f_i^{eq} is defined, for a CDE, by

$$f_i^{eq}(\vec{x}, t) = t_i U(\vec{x}, t) \left(1 + \frac{\vec{\alpha}_j^T \cdot \vec{v}_i}{c_s^2} \right), \quad (70)$$

where the lattice weights t_i and the sound speed c_s of a D2Q9 lattice are defined by

$$t_i = \begin{cases} \frac{4}{9} & \text{if } i = 0 \\ \frac{1}{9} & \text{if } i = 1, 2, 3, 4 \\ \frac{1}{36} & \text{if } i = 5, 6, 7, 8 \end{cases} \quad , \quad c_s^2 = \sum_{i=0}^{8} t_i v_{i,x}^2 = \frac{\lambda^2}{3}. \tag{71}$$

Fig. 9 shows the relative error (67) for the MRT and SRT LB schemes. The relative error is plotted up to different value of Δt after $t_f / \Delta t$ temporal iterations, where $t_f = 10^2$ is the final time. Increasing Δt from 0.1 to 0.5 makes the SRT LB scheme unstable whereas the free parameters of the MRT LB scheme (s_6, s_7, s_8, α_{q_x}, α_{q_y}, and α_χ) allow to ensure stability [15].

6. Conclusion

We have shown in this paper how to derive equivalent PDE up to the second order from MRT D2Q9 LB schemes that aim to simulate CDEs possibly with non-constant advection velocity and non-zero source term. When the advection velocity is constant and without source term, von Neumann analysis was performed on the MRT D2Q9 LB scheme to determine the stability region with respect to the Péclet and Courant numbers. Moreover, well-chosen LB parameters give a numerical convergence rate of three.

Application to marine radar image processing has been presented involving a CDE with non-constant advection velocity and non-linear reaction term. These application shows that such MRT LB schemes are relevant in this context, whereas SRT LB schemes fail to be stable.

Future works will be devoted to obtaining MRT LB schemes exact at the second order in the general case of non-constant advection velocity and non-zero source term.

CRediT authorship contribution statement

The authors contributed equally to this paper.

Declaration of competing interest

The authors declare that they have no known competing financial interests or personal relationships that could have appeared to influence the work reported in this paper.

Data availability

The authors do not have permission to share data.

Acknowledgements

References

[1] S.M. Allen, J.W. Cahn, A microscopic theory for antiphase boundary motion and its application to antiphase domain coarsening, Acta Metall. 27 (6) (1979) 1085–1095.

[2] R. Benzi, S. Succi, M. Vergassola, The lattice Boltzmann equation: theory and applications, Phys. Rep. 222 (3) (1992) 145–197.

[3] B.M. Boghosian, F. Dubois, B. Graille, P. Lallemand, M.M. Tekitek, Unexpected convergence of lattice Boltzmann schemes, Comput. Fluids 172 (2018) 301–311.

[4] Z. Chai, T.S. Zhao, Lattice Boltzmann model for the convection-diffusion equation, Phys. Rev. E 87 (6) (2013) 063309.

[5] S. Chapman, T.G. Cowling, D. Park, The mathematical theory of non-uniform gases, Am. J. Phys. 30 (5) (1962) 389.

[6] J. Chen, Z. Chai, B. Shi, W. Zhang, Lattice Boltzmann method for filtering and contour detection of the natural images, Comput. Math. Appl. 68 (3) (2014) 257–268.

[7] B. Chopard, J.L. Falcone, J. Latt, The lattice Boltzmann advection-diffusion model revisited, Eur. Phys. J. Spec. Top. 171 (1) (2009) 245–249.

[8] D. d'Humières, Generalized lattice-Boltzmann equations, in: Rarefied Gas Dynamics: Theory and Simulations, in: AIAA Progress in Aeronautics and Astronautics, vol. 159, 1992, pp. 450–458.

[9] F. Dubois, Third order equivalent equation of lattice Boltzmann scheme, Discrete Contin. Dyn. Syst. 23 (1/2) (2009) 221–248.

[10] T. Gebäck, A. Heintz, A lattice Boltzmann method for the advection-diffusion equation with Neumann boundary conditions, Commun. Comput. Phys. 15 (2) (2014) 487–505.

[11] M. Geier, M. Schönherr, A. Pasquali, M. Krafczyk, The cumulant lattice Boltzmann equation in three dimensions: theory and validation, Comput. Math. Appl. 70 (4) (2015) 507–547.

[12] A. Hagan, Y. Zhao, Parallel 3D image segmentation of large data sets on a GPU cluster, in: Advances in Visual Computing, Springer, Springer Berlin Heidelberg, 2009, pp. 960–969.

[13] M. Hénon, Viscosity of a lattice gas, Complex Syst. 1 (4) (1987) 763–789.

[14] I.V. Karlin, A. Ferrante, H.C. Öttinger, Perfect entropy functions of the lattice Boltzmann method, Europhys. Lett. 47 (2) (1999) 182.

[15] P. Lallemand, L.S. Luo, Theory of the lattice Boltzmann method: dispersion, dissipation, isotropy, Galilean invariance, and stability, Phys. Rev. E 61 (6) (2000) 6546–6562.

[16] Q. Li, Z. Chai, B. Shi, Lattice Boltzmann model for a class of convection-diffusion equations with variable coefficients, Comput. Math. Appl. 70 (4) (2015) 548–561.

[17] L. Li, R. Mei, J.F. Klausner, Lattice Boltzmann models for the convection-diffusion equation: D2Q5 vs D2Q9, Int. J. Heat Mass Transf. 108 (2017) 41–62.

[18] J. Michelet, L. Mascarilla, H. Chandran, M. Berthier, Geometric segmentation of sea clutter in coherent radar images: range-Doppler map versus range-time intensity map, IEEE Trans. Aerosp. Electron. Syst. 57 (4) (2021) 2278–2287.

[19] K.L. Nguyen, Modèles de champ de phase et modèles lattice Boltzmann pour la segmentation 3D de tumeurs en imagerie ultrasons hautes fréquences, PhDThesis, Université de La Rochelle, 2019.

[20] K.L. Nguyen, M.M. Tekitek, P. Delachartre, M. Berthier, Multiple relaxation time lattice Boltzmann models for multigrid phase-field segmentation of tumors in 3D ultrasound images, SIAM J. Imaging Sci. 12 (3) (2019) 1324–1346.

[21] B. Servan-Camas, F.T.-C. Tsai, Lattice Boltzmann method with two relaxation times for advection–diffusion equation: third order analysis and stability analysis, Adv. Water Resour. 31 (8) (2008) 1113–1126.

[22] B. Shi, Z. Guo, Lattice Boltzmann model for nonlinear convection-diffusion equations, Phys. Rev. E 79 (1) (2009) 016701.

[23] Z. Wang, Z. Yan, Y. Qian, G. Chen, Lattice Boltzmann model of anisotropic diffusion for image denoising, in: 2010 IEEE Youth Conference on Information, Computing and Telecommunications, IEEE, nov 2010, pp. 21–24.

[24] Z. Wang, Z. Yan, G. Chen, Lattice Boltzmann method of active contour for image segmentation, in: 2011 Sixth International Conference on Image and Graphics, IEEE, 2011, pp. 338–343.

[25] X. Xiang, Z. Wang, B. Shi, Modified lattice Boltzmann scheme for nonlinear convection diffusion equations, Commun. Nonlinear Sci. Numer. Simul. 17 (6) (2012) 2415–2425.

[26] Y. Zhao, GPU-accelerated surface denoising and morphing with lattice Boltzmann scheme, in: 2008 IEEE International Conference on Shape Modelling and Applications, IEEE, IEEE, 2008, pp. 19–28.